Numerical Simulations of Supersonic Leading-Edge Receptivity

Shoji Sakaue, Michio Nishioka
Osaka Prefecture University, Sakai, Osaka, 599-8531, Japan

The receptivity of supersonic boundary layer to time periodic Mach wave incident onto leading-edge is examined numerically at a freestream Mach number 2.2 and 4.5. When the Mach wave is coming from below the boundary layer plate, the excited flow is found to be governed by the T-S wave in the upper side boundary layer, and by the forced waves in the lower side boundary layer that are due to the forcing field dominated by pressure waves traveling at $1\pm1/M$.

Key Words: *Supersonic boundary layer instability, Boundary layer receptivity, Laminar flow control*

1. Introduction

The present study is concerned with the receptivity process in supersonic boundary layer flow. Here, the receptivity means the flow process by which external disturbances generate T-S waves. For supersonic flow, many investigations have been carried out through theoretical[1~4], experimental[5~7] and numerical[8~11] approach for boundary layer receptivity to incident Mach waves. However, the supersonic boundary layer receptivity has not been clarified yet. This is mainly because, when the oscillating Mach wave is incident into boundary layer, the forced wave appears and persists long to make the excited flow complex. And in most cases of experimental and numerical investigations, it is concluded, only from the phase velocity of the excited fluctuations, that T-S waves appear. However, the wave length and phase velocity of forced waves are almost the same order as that of T-S waves, so that, it is hard to decompose the T-S waves from the excited fluctuations.

In this paper, we consider the flow near leading-edge of two-dimensional flat-plate placed in supersonic stream at Mach number M=2.2 and 4.5, and the responses of supersonic boundary layer to time periodic Mach waves incident onto the leading-edge is examined through DNS.

2. Numerical schemes

The flow fields are governed by the compressible N-S equations, non-dimensionalized with free stream velocity U_1, density ρ_1 and viscosity μ_1. The origin of the coordinates is set on the leading-edge of the plate, the x-axis is in the streamwise direction and the y-axis normal to the wall. The N-S equations are solved numerically by the third-order upwind TVD scheme for the convection terms and the second-order central difference scheme for the other spatial derivatives. For time advancement, the explicit second-order scheme is used.

3. Leading-edge receptivity at M=2.2

In this section, we consider the flow at freestream Mach number M=2.2. The displacement thickness δ_1 at downstream boundary is selected as the reference length, the computational domain is $-24\le x\le 60$, $-21\le y\le 21$, and the Reynolds number is 974. The fluctuation is assumed to be small and periodic with nondimensional angular frequency ω=0.379. The localized disturbance source which radiates the oscillating Mach wave is placed at x = -47, y=-24, and the leading-edge of the plate is located on the Mach line drawn from this disturbance source. For T-S wave with ω=0.379, the eigenvalue α is 0.5420 + i0.4407×10^{-2} at x=60, corresponding wavelength λ being 11.592, and λ varies from 10.595 (at x=10) to 11.592 (at x=60).

First of all, we show the external disturbance fields. Fig.1 show the instantaneous pressure fluctuations for the case where the flow is assumed to be invisid. The result calculated from the potential flow theory in (a) and the simulation result in (b) are compared. In the present study, the plate thickness is zero, the potential flow theory can be solved easily and very useful for checking the accuracy of the invisid numerical simulation. As seen from these figures, both results are in very good agreement. And as compared with the viscous flow simulation (see fig.2 (a)), it is found that the both results are similar except for the boundary layer region, so that, the invisid flow fluctuation fields on the wall can be considered as the external disturbances forced onto the boundary layer. To estimate the wave number spectrum of u-fluctuation on the wall, it is found that there appear

two dominant waves with the phase velocity 1+1/M and 1-1/M (see fig.4). In the upper side, the intensity of u-fluctuation at the leading-edge region is about 3 to 5 times larger than that at downstream x, say, $x \geq 20$. However, in the lower side, the intensity of u-fluctuation at the leading-edge is as large as in the downstream.

Next, we show the boundary layer responses to the external disturbances. Fig.2 show the instantaneous (a) pressure and (b) vorticity fluctuation fields. Fig.3 plot the amplitude and phase of vorticity fluctuations on the wall against x, in which, solid lines show the T-S wave behavior predicted from the linear stability theory. As seen from these figures, when the Mach wave is coming from below the plate, the excited fluctuation in the upper

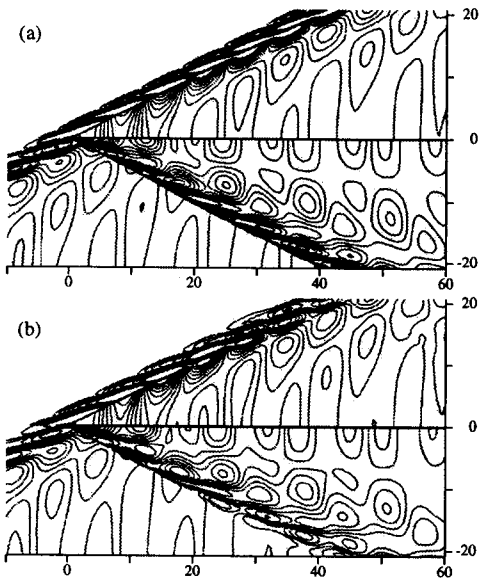

Figure 1 Instantaneous pressure fluctuation field for invisid flow: (a) small perturbation flow theory, (b) numerical simulation result (Euler eq.).

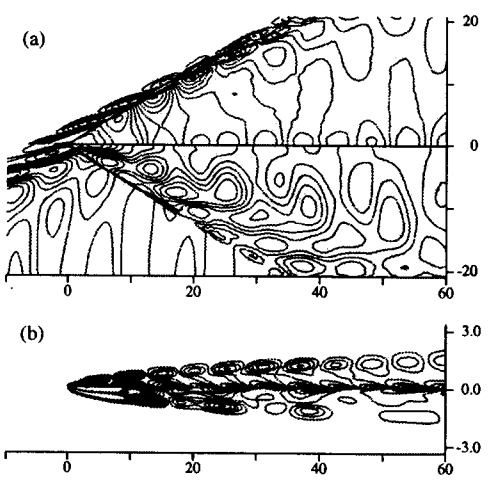

Figure 2 Boundary layer response to Mach wave incident onto leading-edge for M=2.2: (a) pressure fluctuation, (b) vorticity fluctuation.

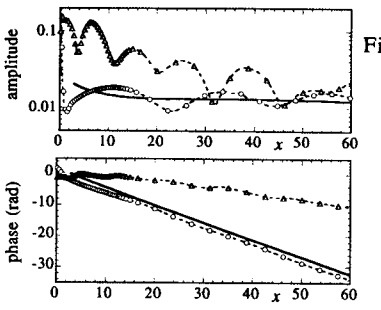

Figure 3 RMS-amplitude and phase of vorticity fluctuation at y=0 against x (○:upper, △:lower). Solid lines represent T-S wave behaviour predicted from liner stability theory.

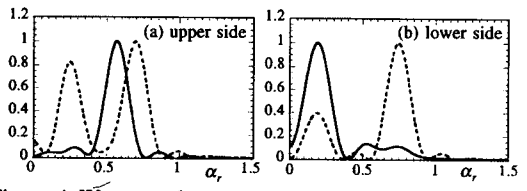

Figure 4 Wave number spectrum of vorticity fluctuation at $15 \leq x \leq 45$, y=0. Dashed lines represent the spectrum of invisid flow u-fluctuation at y=0.

side boundary layer is found to be T-S wave, and it is also confirmed that the wave structure develops into that of the T-S wave at about one wavelength downstream from the leading-edge. The maximum u-fluctuation of the T-S wave is 0.1% of U_1 at x=10, which is almost the same order as that of the incident Mach waves. However, in the lower side boundary layer, the amplitude and phase distributions do not agree with the stability theory, so that, T-S wave dose not exist or is too weak to be detected. The maximum intensity of u-fluctuation in the lower side boundary layer is 1% of U_1 at the leading-edge. In order to identify the fluctuation, fig.4 plots the wave number spectrum contained in the vorticity fluctuation, examined for $15 \leq x \leq 45$, in which dashed lines show the spectrum of invisid flow u-fluctuation at y=0. In the upper side boundary layer, the wave number of the dominant fluctuation is 0.57, which is correspond to the T-S wave. In the lower side, the fluctuation with the wave number 0.21 is dominant, which is correspond to the disturbance with the phase velocity 1+1/M, that is, one of two dominant modes of external disturbance.

4. Leading-edge receptivity at M=4.5

In this section, we consider the high Mach number flow (M=4.5). The computational domain is $-5.0 \leq x \leq 20$, $-8.0 \leq y \leq 8.0$ (the reference length is the displacement thickness at downstream boundary), and the Reynolds number is 2590. The disturbance source is placed at x = -40, y=-8, the leading-edge of the plate is also located on the Mach line drawn from this disturbance source. Fig. 5 shows the results of linear stability analysis for M=4.5,

the amplification rate plotted against the frequency. For M=4.5, the so-called second mode is expected to grow. In this study, we have selected two frequencies; the one is ω=0.8 (T-S mode), and the other is ω=2.4 (second mode). The eigenvalues for each frequencies at x=15 are summarized below.

$\omega = 0.8$: $\alpha = 0.9391+i0.6362\times10^{-2}$ $\lambda = 6.687$

$\omega = 2.4$: $\alpha = 2.6534-i0.2987\times10^{-1}$ $\lambda = 2.367$

Fig.6 and fig.7 show the instantaneous (a) pressure and (b) vorticity fluctuations. Fig.6 is for the case ω=0.8 and fig.7 is for ω=2.4. As seen from these figures, the fluctuations in both sides of the plate are periodic. For ω=0.8, the intensity of vorticity fluctuations at the generalized inflection point, which is near the outer edge of the boundary layer, is larger than that at the wall. While for ω=2.4, the intensity of the vorticity fluctuation on the wall is almost same order as that at the generalized inflection point. Fig.8 and fig.9 show the comparison on the streamwise variations of amplitude and phase of vorticity fluctuations on the wall between simulation results and corresponding stability theory. Fig.8 is for ω=0.8 and fig.9 is for ω=2.4. Solid lines show the wave behavior predicted from linear stability theory. As seen from fig.8 (ω=0.8), in the upper side boundary layer, both results are in good agreements. However, in the lower side, both results do not agree well and the amplitude distribution of simulation result is undulating. For ω=2.4 (fig.9), the phase distributions in both sides of the plate are slightly different from the stability theory. In order to identify the excited fluctuations, the wave number spectrums are estimated by the discrete Fourier transform for $5\leq x\leq 18$. Fig.10 show the wave number spectrum contained in the vorticity fluctuations on the wall for (a) ω=0.8 and (b) ω=2.4, in which dashed lines represent the wave number spectrum of invisid flow u-fluctuations on the wall, as external disturbances. For ω=0.8, the dominant fluctuation in the upper side boundary layer is wave number α=0.86, that is, the excited fluctuation is found to be T-S wave. While in the lower side, there are two dominant waves with wave number being 0.53 and 1.06, which correspond to the external disturbances. For ω=2.4, in the upper side boundary layer, the dominant fluctuation is α=2.27, which is corresponding to the second mode disturbance. In the lower side, there are also two dominant waves. One of which with α=1.78 is corresponding to the external disturbance, and the other α=2.37 is corresponding to the second mode disturbance. So that, in the lower side boundary layer, not only the forced wave but also the second mode disturbance become dominant. Table 1 summarizes the results for the

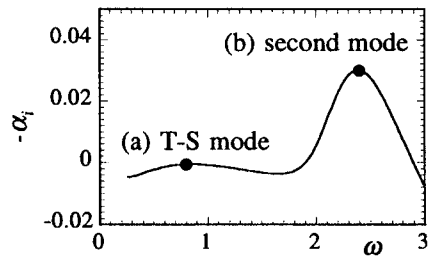

Figure 5 Result of the linear stability analysis for M=4.5.

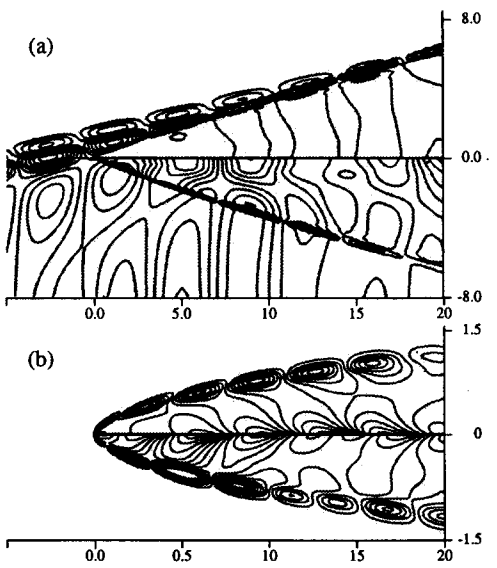

Figure 6 Boundary layer response to Mach wave incident onto leading-edge for M=4.5, ω=0.8: (a) pressure fluctuation, (b) vorticity fluctuation.

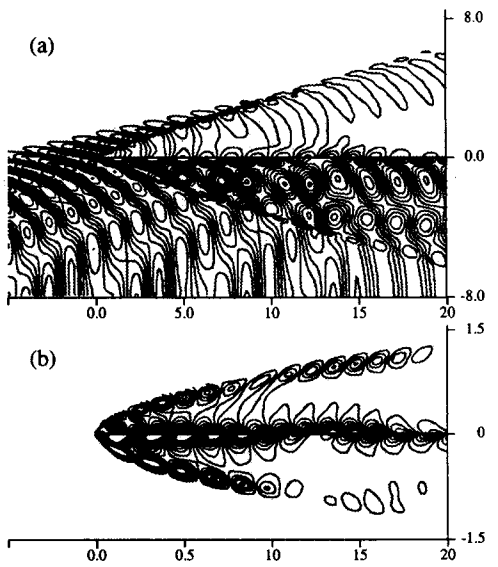

Figure 7 Boundary layer response to Mach wave incident onto leading-edge for M=4.5, ω=2.4: (a) pressure fluctuation, (b) vorticity fluctuation.

intensity of u-fluctuation of the excited fluctuations in boundary layer and the external forcing fields, and it is found that, for the case of M=4.5, the results are almost the same as that obtained for M=2.2.

5. Conclusion

The responses of the supersonic boundary layer at freestream Mach number M=2.2 and M=4.5 to time periodic Mach waves incident onto leading-edge of the plate through direct numerical simulations. When the Mach wave coming from below the plate, in the upper side boundary layer, the intensity of external disturbance at the leading-edge is much larger than that at the downstream region, so that the T-S wave or second mode disturbance excited at the leading-edge can be dominant. The intensity of the excited u-fluctuations is almost the same order as that of incident Mach waves. In the lower side boundary layer, however, the intensity of the external disturbance in the downstream region is as large as at the leading-edge and the flow is governed by the forced wave due to the forcing field in the freestream along the boundary layer. The intensity of excited u-fluctuations is about 3 to 8 times larger than that of the incident Mach waves.

Acknowledgments

This work is supported by the Japanese Ministry of Education, Science and Culture, under a Grant-in-Aid for Encouragement of Young Scientist (No. 12750812).

Reference

1. L. M. Mack (1987) AGARD Rep. No.709.
2. P. W. Duck (1990) J. Fluid Mech. **219**, 423-448.
3. A.V. Fedorov, A.P. Khokhlov (1991) Fluid Dyn. **26**, 4, 531-537.
4. A.V. Fedorov, A.P. Khokhlov (1992) Fluid Dyn. **27**, 1, 29-34.
5. J. M. Kendall (1975) AIAA J. **13**, 3, 290-299.
6. A. D. Kosinov, A. A. Maslov and N. V. Semionov (1996) J. Applied Mech. and Tech. Phys. **38**, 1, 45-51.
7. A. A. Maslov, A. N. Shiplyuk, A. A. Sidorenko and D. Arnal (1998) Russian Academy of Sci., Preprint No.1-98.
8. X. Zhong (1997) AIAA 97-0756.
9. X. Zhong, H. Dong (1999) AIAA 99-0409.
10. M. Malik (1999) IUTAM Symposium on Laminer-Turbulent Transition.
11. Sakaue, S., Nishioka, M. (1999) IUTAM Symposium on Laminer-Turbulent Transition.

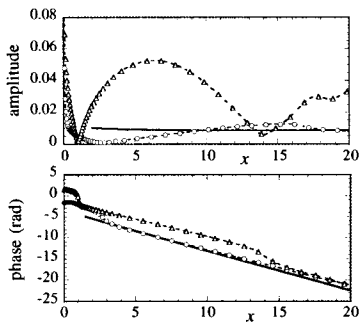

Figure 8 RMS-amplitude and phase of vorticity fluctuation at y=0 against x for M=4.5, ω=0.8(○ :upper, △:lower). Solid lines represent T-S wave behaviour predicted from liner stability theory.

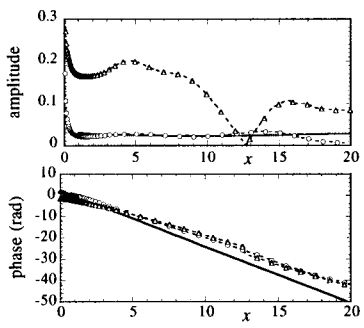

Figure 9 RMS-amplitude and phase of vorticity fluctuation at y=0 against x for M=4.5, ω=2.4(○ :upper, △:lower). Solid lines represent T-S wave behaviour predicted from liner stability theory.

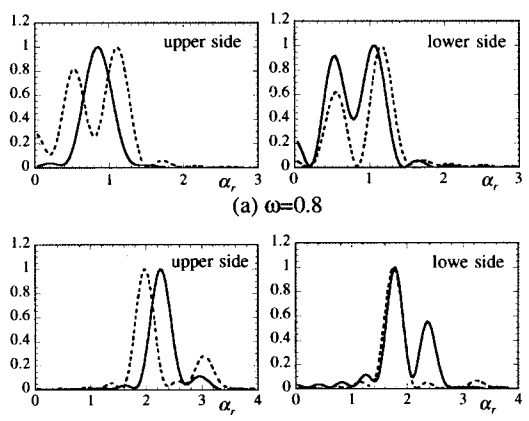

Figure 10 Wave number spectrum of vorticity fluctuation at $5 \le x \le 18$, y=0 for M=4.5; (a) ω=0.8, (b) ω=2.4. Dashed lines represent the spectrum of invisid flow u-fluctuation at y=0.

Table 1 Intensity of the external disturbance and the boundary layer response for M = 4.5, represented by nondimensional rms u-fluctuations (u'/U_1).

	external disturbance	
	$\omega = 0.8$	$\omega = 2.4$
leading-edge	1.8×10^{-3}	1.4×10^{-3}
upper	$4.0\sim6.0 \times 10^{-4}$	$4.0\sim6.7 \times 10^{-4}$
lower	$1.3\sim3.2 \times 10^{-3}$	$3.5\sim5.0 \times 10^{-3}$
	boundary layer fluctuation	
	$\omega = 0.8$	$\omega = 2.4$
upper	$1.5\sim2.5 \times 10^{-4}$	$0.5\sim2.5 \times 10^{-3}$
lower	$5.0\sim8.0 \times 10^{-3}$	$7.0\sim1.1 \times 10^{-2}$